A Gurson-type "layer model" for ductile porous solids with isotropic and kinematic hardening

Léo Morin[a], Jean-Claude Michel[b], Jean-Baptiste Leblond [c]

a. PIMM, Arts et Métiers-ParisTech, CNAM, CNRS, UMR 8006, 151 bd de l'Hôpital, 75013 Paris, France (leo.morin@ensam.eu)
b. Laboratoire de Mécanique et d'Acoustique, CNRS, UPR 7051, Aix-Marseille Univ, Centrale Marseille, 4 impasse Nikola Tesla, CS 40006, 13453 Marseille Cedex 13, France
c. Sorbonne Universités, Université Pierre et Marie Curie (UPMC), CNRS, UMR 7190, Institut Jean Le Rond d'Alembert, F-75005 Paris, France

Résumé :

Le but de ce travail est de proposer un modèle de type Gurson pour les matériaux poreux ductiles avec écrouissage isotrope et cinématique. La dérivation est basée sur une "analyse limite séquentielle" d'une sphère creuse constituée d'un matériau rigide écrouissable. L'hétérogénéité de l'écrouissage est prise en compte en discrétisant la celulle élémentaire en un nombre fini de couches sphériques dans lesquelles les quantités caractérisant l'écrouissage sont supposées homogènes. Le modèle est évalué par comparaison de ses prédictions avec les résultats d'analyses micromécaniques par éléments finis sur les mêmes cellules élémentaires. Les surfaces de charge numériques et théoriques sont notamment comparées pour des distributions initiales de pré-écrouissage isotrope et cinématique. Les prédictions du modèle sont en très bon accord avec les résultats des calculs numériques.

Abstract :

The aim of this work is to propose a Gurson-type model for ductile porous solids exhibiting isotropic and kinematic hardening. The derivation is based on a "sequential limit-analysis" of a hollow sphere made of a rigid-hardenable material. The heterogeneity of hardening is accounted for by discretizing the cell into a finite number of spherical layers in each of which the quantities characterizing hardening are considered as homogeneous. The model is assessed through comparison of its predictions with the results of some micromechanical finite element simulations of the same cell. The numerical and theoretical overall yield loci are compared for given distributions of isotropic and kinematic pre-hardening. A very good agreement between model predictions and numerical results is found.

Keywords : Porous ductile solids ; Isotropic hardening ; Kinematic hardening ; Sequential limit-analysis

1 Introduction

The failure of metals is one of the most challenging problems faced by the scientific and industrial communities. In particular, a difficult but essential task consists in providing predictive micromechanically-based models that permit to account for both monotonic and cyclic loadings.

In the case of *ductile* materials, failure essentially takes place in three steps [1] : (i) the nucleation of voids, (ii) their growth, change of shape and rotation, and finally (iii) their coalescence leading to final failure. The modelling of these mechanisms started with the pioneering work of Gurson [2] who combined homogenization and limit-analysis of a hollow sphere made of a rigid-ideal-plastic isotropic material to derive a model of ductile materials incorporating void growth. Followed by many extensions [3–9] this approach has met considerable success in the reproduction of experimental tests of failure of ductile materials under *monotonic* loading conditions.

The failure of ductile metals under *cyclic* loadings, however, is less well understood and mastered. Experiments have shown that the strain to fracture is considerably lower, for a given load, if it is reached under cyclic conditions rather than monotonically. This reduction of ductility is commonly attributed to an effect of gradual increase of the mean porosity (volume fraction of voids) during each cycle termed the *ratcheting of the porosity*. Devaux et al. [10] showed that Gurson's classical model [2] does not predict the effect of ratcheting of the porosity under cyclic loadings, but a stabilization of the evolution of the porosity right from the first semi-cycle. The explanation of this shortcoming of Gurson's model lies in the crude modelling of strain hardening within this model, and more specifically in the fact that the same "average yield stress of the matrix" appears in both the "square" and the "cosh" terms of the yield function. Only a few models have been proposed in order to account for the heterogeneity of hardening only in the context of isotropic hardening [11, 12].

The importance of the effect of strain hardening upon ductile failure - and especially the ratcheting of the porosity under cyclic loadings - acts as a strong incentive to develop models accounting better for the heterogeneous distribution of hardening in the plastic matrix. In particular, the incorporation of kinematic hardening appears to be necessary in order to deal with cyclic plasticity. The aim of this work is to derive a Gurson-type model accounting for both isotropic and kinematic hardening.

2 A Gurson-type model accounting for isotropic and kinematic hardening

2.1 Position of the problem

Geometry and material. In order to derive the overall constitutive law of the porous medium, we consider, following [2], a spherical "elementary cell" Ω containing a concentric spherical void ω. The porosity (void volume fraction) is defined by $f = \mathrm{vol}(\omega)/\mathrm{vol}(\Omega) = a^3/b^3$, where a is the void's radius and b the cell's external radius.

The material is assumed to be rigid-plastic (no elasticity) and exhibit a mixed, isotropic and kinematic

hardening ; it is thus supposed to obey the following criterion :

$$\phi(\boldsymbol{\sigma}(\mathbf{x})) = (\boldsymbol{\sigma}(\mathbf{x}) - \boldsymbol{\alpha}(\mathbf{x}))^2_{\text{eq}} - \bar{\sigma}^2(\mathbf{x}) \leq 0, \qquad \forall \mathbf{x} \in \Omega - \omega, \tag{1}$$

where $\bar{\sigma}$ is the current yield stress and $(\boldsymbol{\sigma} - \boldsymbol{\alpha})^2_{\text{eq}}$ is defined by

$$(\boldsymbol{\sigma} - \boldsymbol{\alpha})^2_{\text{eq}} = \frac{3}{2}(\boldsymbol{\sigma}' - \boldsymbol{\alpha}) : (\boldsymbol{\sigma}' - \boldsymbol{\alpha}). \tag{2}$$

In this expression, $\boldsymbol{\sigma}' = \boldsymbol{\sigma} - \frac{1}{3}(\operatorname{tr}\boldsymbol{\sigma})\,\mathbf{I}$ (where $\mathbf{I}$ is the second-order unit tensor) is the deviator of $\boldsymbol{\sigma}$, and $\boldsymbol{\alpha}$ is a traceless backstress tensor due to kinematic hardening.

Sequential limit-analysis. Limit-analysis combined with Hill-Mandel homogenization is a convenient framework to derive constitutive equations for porous ductile solids. It permits to effectively operate the scale transition by evidencing the effects of microstructural features at the macroscopic scale.

Yang [13] heuristically extended the methods and results of classical limit-analysis by incorporating the effects of strain hardening and geometric changes. The idea is, still disregarding elasticity, to consider a hardenable material as the sequence of different, successive rigid-ideal plastic materials. At a given instant, a hardenable material without elasticity behaves, if the hardening and the geometry are considered as fixed, like a rigid-ideal plastic material with some pre-hardening modifying its yield criterion and flow rule. An instantaneous limit-load can thus be determined using the classical limit-analysis theorems. In order to account for changes of the strain hardening and geometry, the local hardening parameters and present positions are then updated approximately using the trial velocity field used in the limit-analysis, integrated in a small time step.

Sequential limit-analysis can thus be used to derive a Gurson-type model incorporating both isotropic and kinematic hardening. Hardening will be introduced locally in the criterion as a fixed pre-hardening, and the resulting instantaneous loads promoting plastic flow of the cell will be evaluated.

2.2 Macroscopic plastic potential

To approximately calculate the macroscopic plastic potential, we consider [2]'s trial incompressible velocity field. The macroscopic plastic potential is given by

$$\Pi(\mathbf{D}) = \frac{1}{\text{vol}(\Omega)} \int_{\Omega-\omega} (\bar{\sigma} d_{\text{eq}} + \boldsymbol{\alpha} : \mathbf{d}) \, \mathrm{d}\Omega = \Pi^{\text{iso}}(\mathbf{D}) + \Pi^{\text{kine}}(\mathbf{D}), \tag{3}$$

where the "isotropic" and "kinematic" contributions $\Pi^{\text{iso}}(\mathbf{D})$ and $\Pi^{\text{kine}}(\mathbf{D})$ to $\Pi(\mathbf{D})$ are given by

$$\begin{cases} \Pi^{\text{iso}}(\mathbf{D}) &= \dfrac{1}{\text{vol}(\Omega)} \displaystyle\int_{\Omega-\omega} \bar{\sigma} d_{\text{eq}} \, \mathrm{d}\Omega \\ \Pi^{\text{kine}}(\mathbf{D}) &= \dfrac{1}{\text{vol}(\Omega)} \displaystyle\int_{\Omega-\omega} \boldsymbol{\alpha} : \mathbf{d} \, \mathrm{d}\Omega. \end{cases} \tag{4}$$

One necessary assumption to evaluate these integrals analytically will be that the local hardening pa-

rameters are distributed in a certain, specific way within the matrix. The cell is thus considered to be composed of a finite number N of phases distributed in concentric spheres of radii (see Figure 1)

$$a = r_1 < ... < r_i < ... < r_{N+1} = b. \tag{5}$$

The phase contained within the interval $[r_i, r_{i+1}]$ is denoted P_i.

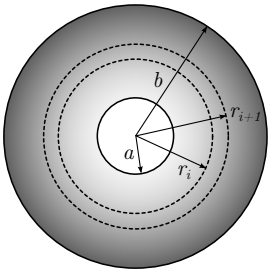

FIGURE 1 – Hollow sphere : definition of some geometric parameters.

Isotropic potential. In order to calculate the potential $\Pi^{\text{iso}}(\mathbf{D})$, we introduce the following approximation on the spatial distribution of the yield limit $\bar{\sigma}$:

$\mathcal{A}_1$: *In each phase P_i, the yield limit $\bar{\sigma} = \bar{\sigma}^i$ is considered as uniform.*

The expression of the partial isotropic potential then becomes

$$\Pi^{\text{iso}}(\mathbf{D}) = \sum_{i=1}^{N} \Pi_i^{\text{iso}}(\mathbf{D}), \tag{6}$$

where

$$\begin{aligned}\Pi_i^{\text{iso}}(\mathbf{D}) &= \bar{\sigma}^i \int_{1/f_{i+1}}^{1/f_i} \sqrt{D_{\text{eq}}^2 + 4D_{\text{m}}^2 u^2}\, \frac{\mathrm{d}u}{u^2} \\ &= \bar{\sigma}^i \left[-\sqrt{\frac{D_{\text{eq}}^2}{u^2} + 4D_{\text{m}}^2} + 2D_{\text{m}} \ln\left(\frac{2D_{\text{m}} u}{D_{\text{eq}}} + \sqrt{1 + \frac{4D_{\text{m}}^2 u^2}{D_{\text{eq}}^2}} \right) \right]_{u=1/f_{i+1}}^{u=1/f_i}.\end{aligned} \tag{7}$$

In this equation, the "local volume fraction" f_i is given by

$$f_i = \left(\frac{r_i}{b}\right)^3. \tag{8}$$

Kinematic potential. In order to calculate the kinematic part $\Pi^{\text{kine}}(\mathbf{D})$ of the potential, we introduce the following approximation on the spatial distribution of the backstress $\boldsymbol{\alpha}$:

$\mathcal{A}_2$: *In phase P_i, the backstress $\boldsymbol{\alpha}$ is of the form :*

$$\boldsymbol{\alpha} = \boldsymbol{\alpha}^i = \mathbf{A}_1^i + A_2^i(-2\mathbf{e}_r \otimes \mathbf{e}_r + \mathbf{e}_\theta \otimes \mathbf{e}_\theta + \mathbf{e}_\varphi \otimes \mathbf{e}_\varphi), \tag{9}$$

where $\mathbf{A}_1^i$ is a second-order traceless tensor and A_2^i a scalar, both uniform within P_i.

The expression of the kinematic potential then becomes

$$\Pi^{\text{kine}}(\mathbf{D}) = \mathbf{A}_1 : \mathbf{D}' + 3A_2 D_{\text{m}}, \tag{10}$$

where

$$\left\{ \begin{array}{ll} \mathbf{A}_1 & = \displaystyle\sum_{i=1}^{N} \mathbf{A}_1^i (f_{i+1} - f_i) \\ A_2 & = \displaystyle\sum_{i=1}^{N} 2A_2^i \ln\left(\frac{f_{i+1}}{f_i}\right). \end{array} \right. \tag{11}$$

2.3 Macroscopic yield criterion

The macroscopic yield criterion is given by the parametric equation

$$\mathbf{\Sigma} = \frac{\partial(\Pi^{\text{iso}} + \Pi^{\text{kine}})}{\partial \mathbf{D}}(\mathbf{D}) = \mathbf{\Sigma}^{\text{iso}} + \mathbf{\Sigma}^{\text{kine}}, \tag{12}$$

where the "isotropic" and "kinematic" contributions $\mathbf{\Sigma}^{\text{iso}}$ and $\mathbf{\Sigma}^{\text{kine}}$ to the stress $\mathbf{\Sigma}$ are defined by

$$\left\{ \begin{array}{ll} \mathbf{\Sigma}^{\text{iso}} & = \dfrac{\partial \Pi^{\text{iso}}}{\partial \mathbf{D}}(\mathbf{D}) \\ \mathbf{\Sigma}^{\text{kine}} & = \dfrac{\partial \Pi^{\text{kine}}}{\partial \mathbf{D}}(\mathbf{D}). \end{array} \right. \tag{13}$$

Using the previous potentials, one obtains the macroscopic yield locus in the parametric form

$$\left\{ \begin{array}{lcl} \Sigma_{\text{m}} - A_2 & = & \Sigma_{\text{m}}^{\text{iso}}(\xi) \\ (\mathbf{\Sigma} - \mathbf{A}_1)_{\text{eq}} & = & \Sigma_{\text{eq}}^{\text{iso}}(\xi), \end{array} \right. \tag{14}$$

where $\Sigma_{\text{m}}^{\text{iso}}$ and $\Sigma_{\text{eq}}^{\text{iso}}$ are given by

$$\left\{ \begin{array}{ll} \Sigma_{\text{m}}^{\text{iso}} & = \dfrac{1}{3}\dfrac{\partial \Pi^{\text{iso}}}{\partial D_{\text{m}}} = \displaystyle\sum_{i=1}^{N} \Sigma_{\text{m},i}^{\text{iso}} \\ \Sigma_{\text{eq}}^{\text{iso}} & = \dfrac{\partial \Pi^{\text{iso}}}{\partial D_{\text{eq}}} = \displaystyle\sum_{i=1}^{N} \Sigma_{\text{eq},i}^{\text{iso}} \end{array} \right. \tag{15}$$

with

$$\left\{ \begin{array}{ll} \Sigma_{\text{m},i}^{\text{iso}} & = \dfrac{2}{3}\bar{\sigma}^i \left[\ln\left(2\xi u + \sqrt{4\xi^2 u^2 + 1}\right)\right]_{u=1/f_{i+1}}^{u=1/f_i} \\ \Sigma_{\text{eq},i}^{\text{iso}} & = \bar{\sigma}^i \left[-\sqrt{4\xi^2 + \dfrac{1}{u^2}}\right]_{u=1/f_{i+1}}^{u=1/f_i} \end{array} \right. , \quad \xi = \frac{D_{\text{m}}}{D_{\text{eq}}}. \tag{16}$$

3 Assessment of the model

3.1 Description of the simulations

In order to study the macroscopic criterion, we consider all internal parameters (geometry and hardening) as fixed. We thus solve the limit-analysis problem for a given, fixed pre-hardening (resulting from some given prestraining), without any geometry update, using the finite element method (FEM).

Axisymmetric loadings are considered : $\Sigma_{11} = \Sigma_{22} \neq 0$, $\Sigma_{33} \neq 0$, and $\Sigma_{ij} = 0$ otherwise. Two Lode angles (denoted θ_L) are considered : $\theta_L = 0$ corresponding to $\Sigma_{33} - \Sigma_{11} > 0$ and $\theta_L = \pi$ corresponding to $\Sigma_{33} - \Sigma_{11} < 0$. The simulations are performed by solving an elastic-plastic evolution problem, the limit-load being considered as reached when the overall stress components no longer evolve [14].

3.2 Isotropic pre-hardening

We consider two cases with isotropic pre-hardening (and no kinematic pre-hardening : $\boldsymbol{\alpha} = \mathbf{0}$ everywhere in the matrix) :

— *Case 1.* Hardening is assumed to be more important near the cavity ; the yield stress is supposed to vary linearly with r from the value $\bar{\sigma}(r = a) = 1.5\ \bar{\sigma}_0$ to the value $\bar{\sigma}(r = b) = 0.5\ \bar{\sigma}_0$.

— *Case 2.* Hardening is assumed to be more important near the cell's boundary ; the yield stress is supposed to vary linearly with r from the value $\bar{\sigma}(r = a) = 0.5\ \bar{\sigma}_0$ to the value $\bar{\sigma}(r = b) = 1.5\ \bar{\sigma}_0$.

Figure 2 compares the yield surfaces associated to the theoretical model with $N = 10$ phases, [2]'s model without pre-hardening and the finite element results, for a porosity $f = 0.01$.

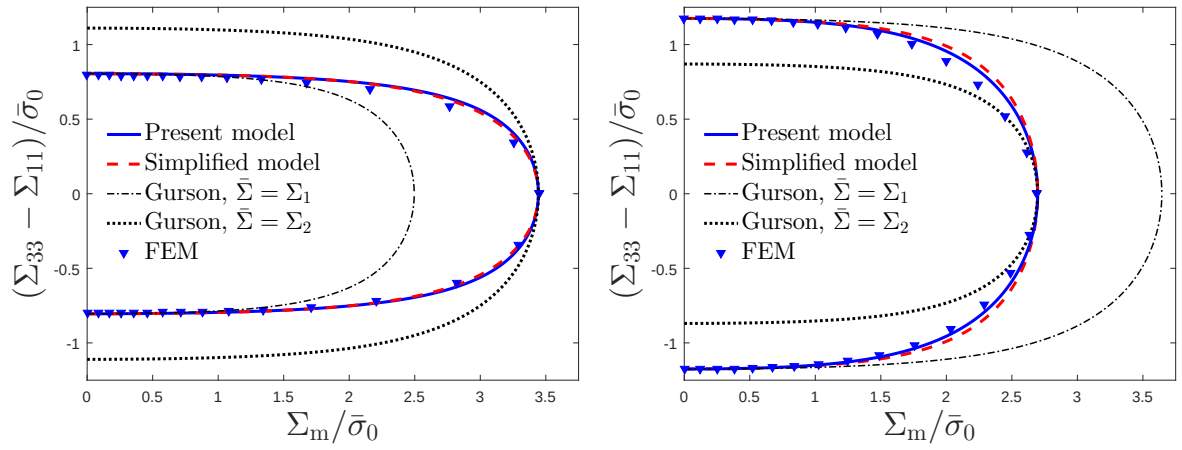

FIGURE 2 – Yield surfaces for isotropic pre-hardening : theoretical model (Present model), Gurson's model (Gurson) and finite element results (FEM). (a) Case 1, (b) Case 2 (see text).

3.3 Kinematic pre-hardening

We now consider three cases with kinematic pre-hardening (and no isotropic pre-hardening : $\bar{\sigma} = \bar{\sigma}_0 = Cst.$ everywhere). In all cases the local backstress $\boldsymbol{\alpha}$ is of the form

$$\boldsymbol{\alpha} = \boldsymbol{\alpha}_1(r) + \alpha_2(r)(-2\mathbf{e}_r \otimes \mathbf{e}_r + \mathbf{e}_\theta \otimes \mathbf{e}_\theta + \mathbf{e}_\varphi \otimes \mathbf{e}_\varphi), \tag{17}$$

where the traceless tensor $\boldsymbol{\alpha}_1(r)$ and the scalar $\alpha_2(r)$ depend only on r.

— *Case 1.* Pre-hardening is assumed to affect the sole deviatoric stress ; the non-zero components of $\boldsymbol{\alpha}_1$ are : $\alpha_{1(11)} = \alpha_{1(22)} = -\alpha_{1(33)}/2 = -\bar{\sigma}_0/6$ and α_2 is nil.

— *Case 2.* Pre-hardening is assumed to affect the sole hydrostatic stress ; α_2 is supposed to vary linearly from the value $\alpha_2(r = a) = -\bar{\sigma}_0/6$ to the value $\alpha_2(r = b) = 0$, and $\boldsymbol{\alpha}_1$ is nil.

— *Case 3.* Pre-hardening is assumed to affect both the hydrostatic and deviatoric stresses ; the non-zero components of $\boldsymbol{\alpha}_1$ are $\alpha_{1(11)} = \alpha_{1(22)} = -\alpha_{1(33)}/2 = -\bar{\sigma}_0/4$, and α_2 is supposed to vary linearly from the value $\alpha_2(r = a) = -\bar{\sigma}_0/4$ to the value $\alpha_2(r = b) = 0$.

Figure 3 compares the yield surfaces associated to the theoretical model with $N = 30$ phases, [2]'s model without pre-hardening (with $\bar{\sigma} = \bar{\sigma}_0$ everywhere in the matrix) and the finite element results, for a porosity $f = 0.01$.

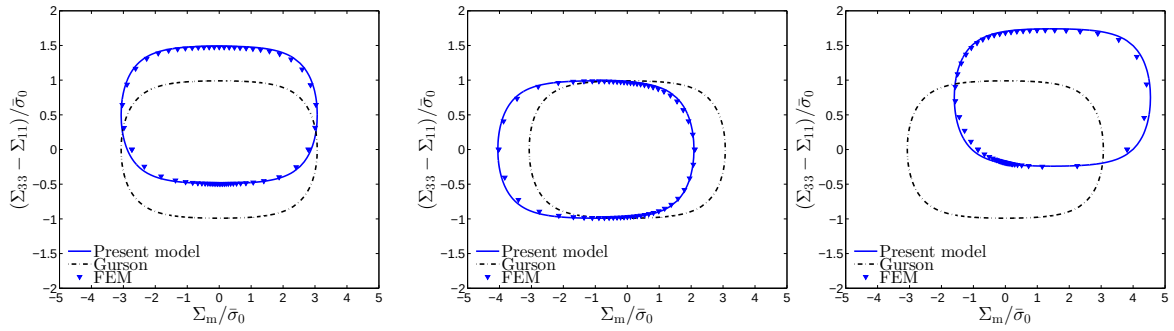

(a) (b) (c)

FIGURE 3 – Yield surfaces for kinematic pre-hardening : theoretical model (Present model), Gurson's model without hardening (Gurson) and finite element results (FEM). (a) Case 1, (b) Case 2, (c) Case 3 (see text).

4 Conclusion

An approximate yield criterion was derived by performing a "sequential limit-analysis" of a hollow sphere made of a rigid-hardenable matrix. To approximately account for the heterogeneity of hardening, the cell was discretized into a finite number of spherically distributed phases in which the quantities characterizing hardening were considered as homogeneous. The macroscopic yield locus was characterized by an overall criterion expressed in a parametric form, wherein the heterogeneous local hardening parameters were accounted for through macroscopic variables.

The model was assessed numerically using micromechanical finite element simulations. Overall yield loci were investigated for both isotropic and kinematic pre-hardening : a very good agreement was observed between the numerical results and the predictions of the model.

Références

[1] A.A. Benzerga and J.B. Leblond. Ductile fracture by void growth to coalescence. *Advances in Applied Mechanics*, 44 (2010), 169–305.

[2] A. L. Gurson. Continuum theory of ductile rupture by void nucleation and growth : Part I-Yield

criteria and flow rules for porous ductile media. *ASME Journal of Engineering Materials and Technology*, 99 (1997), 2–15.

[3] M.Gologanu, J.B. Leblond, and J. Devaux. Approximate models for ductile metals containing non-spherical voids-Case of axisymmetric prolate ellipsoidal cavities. *Journal of the Mechanics and Physics of Solids*, 41 (1993), 1723–1754.

[4] A.A. Benzerga and J. Besson. Plastic potentials for anisotropic porous solids. *European Journal of Mechanics - A/Solids*, 20 (2001), 397–434.

[5] V. Monchiet, O. Cazacu, E. Charkaluk, and D. Kondo. Macroscopic yield criteria for plastic anisotropic materials containing spheroidal voids. *International Journal of Plasticity*, 24 (2008), 1158–1189.

[6] S.M. Keralavarma and A.A. Benzerga. A constitutive model for plastically anisotropic solids with non-spherical voids. *Journal of the Mechanics and Physics of Solids*, 58 (2010), 874–901.

[7] K. Madou and J.B. Leblond. A Gurson-type criterion for porous ductile solids containing arbitrary ellipsoidal voids-I : Limit-analysis of some representative cell. *Journal of the Mechanics and Physics of Solids*, 60 (2012), 1020–1036.

[8] K. Madou, J.B. Leblond, and L. Morin. Numerical studies of porous ductile materials containing arbitrary ellipsoidal voids-II : Evolution of the length and orientation of the void axes. *European Journal of Mechanics - A/Solids*, 42 (2013), 490–507.

[9] L. Morin, J.B. Leblond, and D. Kondo. A Gurson-type criterion for plastically anisotropic solids containing arbitrary ellipsoidal voids. *International Journal of Solids and Structures*, 77 (2015), 86–101.

[10] J. Devaux, M. Gologanu, J. B. Leblond, and G. Perrin. On Continued void growth in ductile metals subjected to cyclic loadings. In J. Willis, editor, *Proceedings of the IUTAM Symposium on Nonlinear Analysis of Fracture*, pp 299–310, 1997.

[11] J.B. Leblond, G. Perrin, and J. Devaux. An improved Gurson-type model for hardenable ductile metals. *European Journal of Mechanics - A/Solids*, 14 (1995), 499–527.

[12] R. Lacroix, J.B. Leblond, and G. Perrin. Numerical study and theoretical modelling of void growth in porous ductile materials subjected to cyclic loadings. *European Journal of Mechanics - A/Solids*, 55 (2016), 100–109.

[13] W. H. Yang. Large deformation of structures by sequential limit analysis. *International Journal of Solids and Structures*, 30 (1993), 1001–1013.

[14] J. C. Michel, H. Moulinec, and P. Suquet. Effective properties of composite materials with periodic microstructure : a computational approach. *Computer Methods in Applied Mechanics and Engineering*, 172 (1999), 109–143.